

Modelling X-ray emitting stationary shocks in magnetized protostellar jets

S. Ustamujic¹, S. Orlando², R. Bonito^{2,3}, M. Miceli^{2,3}, A. I. Gómez de Castro¹, and J. López-Santiago⁴

¹ S. D. Astronomía y Geodesia, Facultad de Ciencias Matemáticas, Universidad Complutense de Madrid, 28040 Madrid, Spain

² INAF-Osservatorio Astronomico di Palermo, Piazza del Parlamento 1, 90134 Palermo, Italy

³ Dipartimento di Fisica e Chimica, Università di Palermo, Via Archirafi 36, 90123 Palermo, Italy

⁴ Dpto. de Astrofísica y CC. de la Atmósfera, Facultad de Física, Universidad Complutense de Madrid, 28040 Madrid, Spain

Abstract

The early stages of a star birth are characterized by a variety of mass ejection phenomena, including outflows and collimated jets that are strongly related to the accretion process developed in the context of the star-disc interaction. Jets move through the ambient medium producing complex structures observed at different wavelengths. In particular, X-ray observations show evidence of strong shocks heating the plasma up to a few million degrees. In some cases, the shocked features appear to be stationary. They are interpreted as shock diamonds. We aim at investigating the physical properties of the shocked plasma and the role of magnetic fields on the collimation of the jet and the formation of a stationary shock. We performed 2.5D MHD simulations modelling the propagation of a jet ramming with a supersonic speed into an initially isothermal and homogeneous magnetized medium and compared the results with observations.

1 Introduction

Usually jets from young stars are revealed by the presence of a chain of knots, known as Herbig-Haro (HH) objects. Some observations show evidence of faint X-ray emitting sources within the jet (e.g. [8, 2, 16, 21, 11, 20]). In some cases, the shocked features appear to be stationary and located close to the base of the jet (e.g. HH154, [9]; DG Tau, [11]). They are interpreted as shock diamonds and have been modeled through hydrodynamic simulations by [3].

The general consensus is that magnetic fields play a fundamental role in launching, collimating and stabilizing the plasma inside jets. In this work, we instead investigate the role of the magnetic field in the formation, stability and detectability in X-rays of stationary shocks by exploring different configurations for the magnetic field. One possible observational key to discriminate between different theories could be the detection of possible signatures of rotation in protostellar jets, as described by several authors ([1, 22, 5, 6]). Alternative interpretations include asymmetric shocking and/or jet precession (e.g., [19, 7]).

In this work we study the formation of quasi-stationary X-ray emitting sources close to the base of protostellar jets through 2.5D MHD simulations. We propose a new MHD model that describes the propagation of a jet through a magnetic nozzle ramming at supersonic speed into an initially isothermal and homogeneous magnetized medium. We compare our results with observations.

2 The model

We model the propagation of a continuously driven protostellar jet through an initially isothermal and homogeneous magnetized medium. We assume that the fluid is fully ionized and that it can be regarded as a perfect gas with a ratio of specific heats $\gamma = 5/3$. The system is described by the time-dependent MHD equations taking into account the radiative losses from optically thin plasma and the magnetic field oriented thermal conduction (including the effects of heat flux saturation). The calculations were performed using PLUTO ([14]), a modular Godunov-type code for astrophysical plasmas.

We adopt a 2.5D cylindrical (r, z) coordinate system, assuming axisymmetry and the jet axis coincident with the z axis. The computational grid size is $r \times z = 300 \times 900$ AU. The mesh is uniformly spaced along the two directions, giving a spatial resolution of 0.5 AU. We follow the evolution for ~ 50 years. These dimensions and time are comparable with observations of jets from young stars. We consider an initially isothermal and homogeneous magnetized medium, with initial temperature and density fixed to $T_a = 100$ K and $n_a = 100 \text{ cm}^{-3}$ respectively. We define a jet with a mass ejection rate of $\sim 10^{-8} M_\odot \text{ yr}^{-1}$, following typical outflow rates found by [4] and [15] for jets from low-mass classical T Tauri stars (CTTS). Our model depend on a number of physical parameters, such as, the magnetic field strength, the jet density, velocity (including a possible rotational velocity v_φ) and radius. We define an initially uniform magnetic field along the z axis of $B_z = 5$ mG, consistent with [18] and with the value estimated by [3]. In models M0_1-M0_3 we also consider the plasma of the jet characterised by an angular velocity corresponding to maximum linear rotational velocities of $v_{\varphi, \text{max}} = 75 - 150 \text{ km s}^{-1}$ at the lower boundary (see Sec. 3.1). The particle number density of the jet is $n_j = 10^4 \text{ cm}^{-3}$ at the lower boundary, decreasing one order of magnitude during jet expansion, which leads to values consistent with those inferred by [2]. The jet velocity is $v_j = 500 \text{ km s}^{-1}$, in good agreement with [10].

Axisymmetric boundary conditions are imposed along the jet axis, a constant inflow (according to the jet initial parameters) at $z = 0$, and outflow boundary conditions are assumed elsewhere.

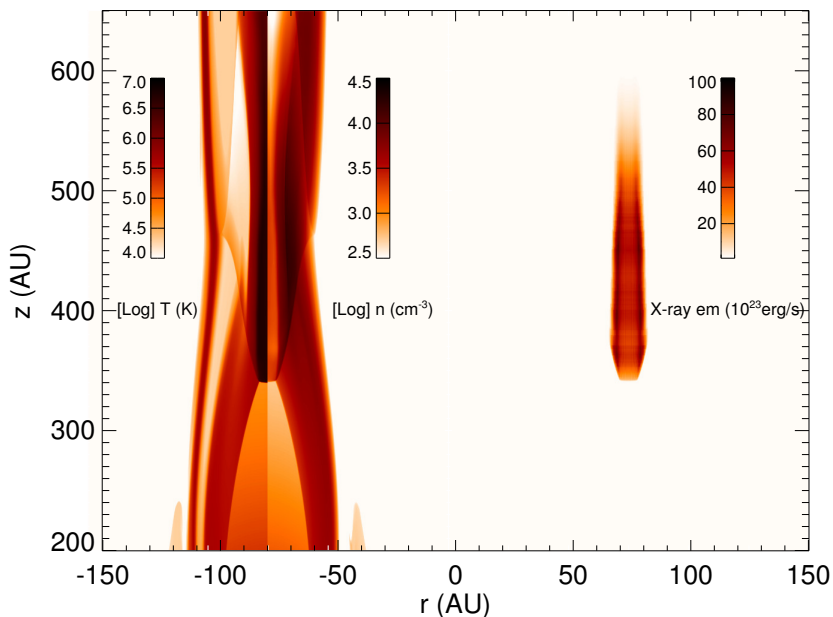


Figure 1: Two-dimensional maps of temperature (left half-panel on the left), density (right half-panel on the left), and spatial distribution of the synthesized X-ray emission (on the right). The animation show $t \approx 40$ years of evolution.

3 Results

In Figure 1 we show the evolution of the shock diamond and report the 2D spatial distributions for temperature, density, and synthesized X-ray emission in the energy range [0.3-10] keV. The incoming jet propagates through the magnetized domain and expands because its dynamic pressure is much larger than the ambient pressure. The jet reaches its maximum expansion at $z \approx 200$ AU and then is gradually collimated by the ambient magnetic field, reaching its minimum cross-section at $z \approx 340$ AU. The flow is compressed forming a diamond shaped structure (see left panel in Fig. 1), composed by oblique shock waves inclined at a given angle with respect to the flow and a normal shock wave perpendicular to the jet. In this simulation the diamond structure forms after ~ 8 years of evolution, and it is stationary for the rest of the simulation ($t \approx 50$ yr). At the shock diamond, the plasma density and temperature reach respective maximum values of $\sim 2 \cdot 10^4 \text{ cm}^{-3}$ and $\sim 6 \cdot 10^6 \text{ K}$. These values are in excellent agreement with the X-ray observations of [8] and [2].

From the 3D spatial distribution of temperature and density reconstructed from the 2.5D simulations, we synthesize the emission in the [0.3-10] keV band to compare our model with observations. In particular we derive 2D X-ray images by integrating the X-ray emission along the line of sight (assumed to be perpendicular to the jet axis). Right panel in Figure 1 shows the spatial distribution of the X-ray emission as a single elongated source corresponding to the shock diamond region. The overall X-ray luminosity is $L_X \approx 9 \cdot 10^{28} \text{ erg s}^{-1}$, compatible with those detected in several HH objects (e.g. [8, 2, 12, 18]).

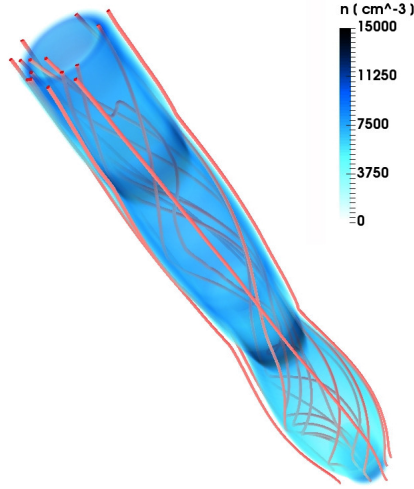


Figure 2: 3D representation of the density distribution and the magnetic field configuration (blue lines) for the model M0.3 after ~ 50 years of evolution.

3.1 Role of the jet rotational velocity

In this section we study the influence of introducing an angular velocity to the jet. We define a constant angular velocity producing maximum linear rotational velocity values, $v_{\varphi, \max}$, of 75-150 km s^{-1} for models M0.1-M0.3 at the lower boundary. Jet rotation causes a toroidal component at the initially axial magnetic field achieving a helicoidal configuration during the simulation, contributing to the jet collimation. In Figure 2 we show a 3D representation of the density distribution and magnetic field configuration for model M0.3, the one with the highest rotational velocity of the cases explored.

Figure 3 shows the spatial distribution of the X-ray emission for the models M0.1, M0.2 and M0.3, derived as explained at the beginning of this section. We find that the X-ray emission source corresponding to the shock diamond is closer to the base of the jet and more extended for models with higher rotational velocities. The X-ray total shock luminosity, L_X , in the [0.3-10] keV band is $1.2 \times 10^{29} \text{ erg s}^{-1}$ for model M0.1, $1.6 \times 10^{29} \text{ erg s}^{-1}$ for model M0.2, and $2.2 \times 10^{29} \text{ erg s}^{-1}$ for model M0.3, consistent with those detected in several HH objects ([8, 2, 12, 18]).

We also calculate the density-weighted average velocity along the line of sight (considering the line of sight perpendicular to the jet axis). We degrade the spatial resolution of the maps derived from the simulations from 0.5 AU to 20 AU (typical average resolution achieved in observations), in order to compare it with the observations. In Figure 4, we show 2D distributions for the density-weighted velocities along the line of sight for the three models. The projected velocities are larger at the edge of the jet, reaching its maximum in proximity of the shock diamond. The velocities derived in the pre-shock region are lower: maximum values for M0.1, M0.2, and M0.3 are ~ 30 , ~ 40 , and $\sim 50 \text{ km s}^{-1}$, respectively. These values are compatible with those inferred from observations by [1] and [22].

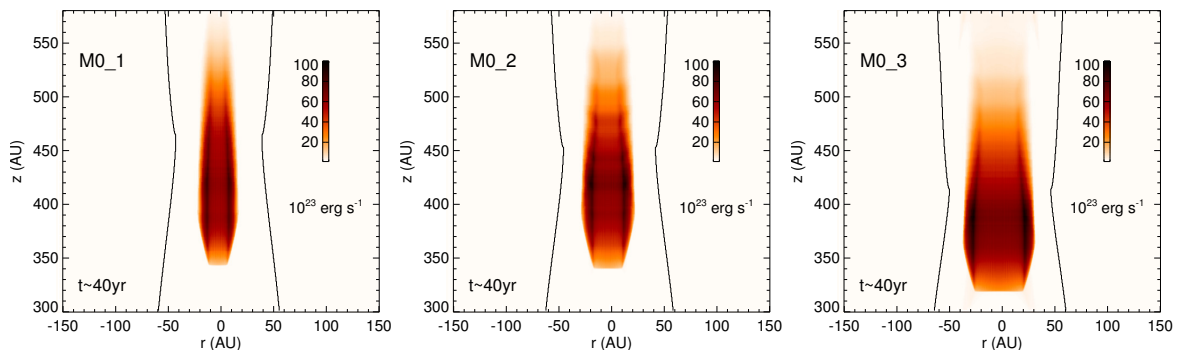


Figure 3: Spatial distribution of the X-ray emission after ~ 40 years of evolution. We compare models M0_1, M0_2 and M0_3.

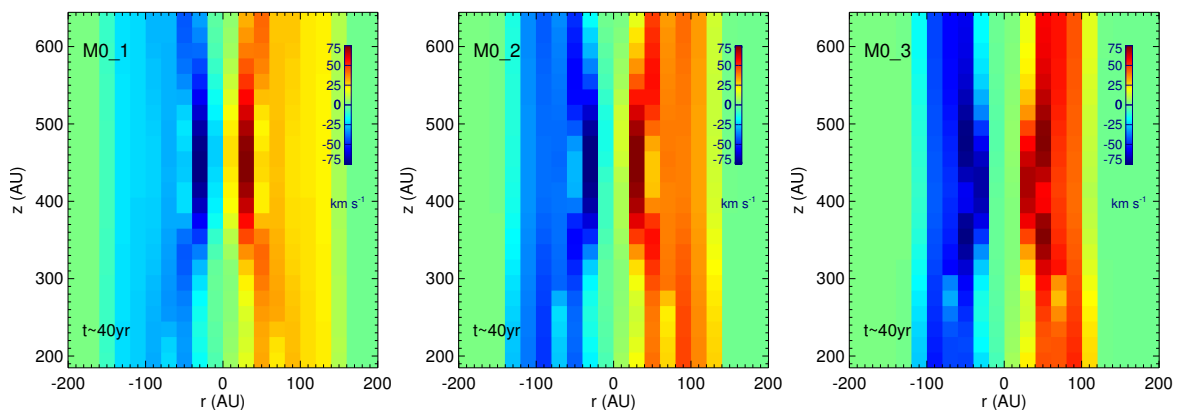


Figure 4: Density-weighted rotational velocity along the line of sight with macropixel resolution of 20 AU after ~ 40 years of evolution. We compare models M0_1, M0_2 and M0_3.

4 Conclusions

We derive the physical parameters of a protostellar jet that can give rise to stationary X-ray sources at the base of the jet consistent with observations of HH objects. We obtain shock temperatures of $\sim 5 \cdot 10^6$ K and luminosities $L_X \approx 10^{29}$ erg s $^{-1}$, in excellent agreement with the results of [8, 2, 12, 18, 13]. We obtain the highest luminosity in model M0_3, the model with the highest jet rotational velocity.

We also investigate the effect of jet rotation on the model. Several detections of gradients in the radial velocity profile across jets from T Tauri stars have been reported in the past. They have been interpreted as signatures of jet rotation around its symmetry axis (e.g. [1, 5, 22]). Those authors derive toroidal velocities in the emitting regions in the range 5 – 30 km s $^{-1}$. We find velocities of 5 – 30 km s $^{-1}$ for model M0_1, 6 – 40 km s $^{-1}$ for model M0_2, and 7 – 50 km s $^{-1}$ for model M0_3 in the pre-shock region. Thus, our model could be a useful tool for the investigation of the still debated rotation of the jets.

After comparing our model results with the observational findings, we conclude that

the model reproduces most of the physical properties observed in the X-ray emission of protostellar jets (temperature, emission measure, X-ray luminosity, etc.). Thus our model provides a simple and natural explanation for the origin of stationary X-ray sources at the base of protostellar jets. The comparison of our MHD model results with the X-ray observations could provide a fundamental tool for investigating the role of the magnetic field on the protostellar jet dynamics and X-ray emission.

Acknowledgments

S.U. acknowledges the hospitality of the INAF Osservatorio Astronomico di Palermo, where part of the present work was carried out using the HPC facility (SCAN). PLUTO is being developed at the Turin Astronomical Observatory in collaboration with the Department of General Physics of the Turin University. This work was supported by grant BES-2012-061750 from the Spanish Government under research project AYA2011-29754-C03-01.

References

- [1] Bacciotti, F., Ray, T. P., Mundt, R., Eisloffel, J., & Solf, J. 2002, *ApJ*, 576, 222
- [2] Bally, J., Feigelson, E., & Reipurth, B. 2003, *ApJ*, 584, 843
- [3] Bonito, R., Orlando, S., Miceli, M., et al. 2011, *ApJ*, 737, 54
- [4] Cabrit, S. 2007, *Star-Disk Interaction in Young Stars*, 243, 203
- [5] Coffey, D., Bacciotti, F., Woitas, J., Ray, T. P., & Eisloffel, J. 2004, *ApJ*, 604, 758
- [6] Coffey, D., Dougados, C., Cabrit, S., Pety, J., & Bacciotti, F. 2015, *ApJ*, 804, 2
- [7] Correia, S., Zinnecker, H., Ridgway, S. T., & McCaughrean, M. J. 2009, *AAP*, 505, 673
- [8] Favata, F., Fridlund, C. V. M., Micela, G., Sciortino, S., & Kaas, A. A. 2002, *AAP*, 386, 204
- [9] Favata, F., Bonito, R., Micela, G., et al. 2006, *AAP*, 450, L17
- [10] Fridlund, C. V. M., Liseau, R., Djupvik, A. A., et al. 2005, *AAP*, 436, 983
- [11] Güdel, M., Skinner, S. L., Briggs, K. R., et al. 2005, *ApJ*, 626, L53
- [12] Güdel, M., Skinner, S. L., Audard, M., Briggs, K. R., & Cabrit, S. 2008, *AAP*, 478, 797
- [13] López-Santiago, J., Bonito, R., Orellana, M., et al. 2015, *APJ*, 806, 53
- [14] Mignone, A., Bodo, G., Massaglia, S., et al. 2007, *ApJ*, 170, 228
- [15] Podio, L., Eisloffel, J., Melnikov, S., Hodapp, K. W., & Bacciotti, F. 2011, *AAP*, 527, A13
- [16] Pravdo, S. H., Tsuboi, Y., & Maeda, Y. 2004, *ApJ*, 605, 259
- [17] Schneider, P. C., & Schmitt, J. H. M. M. 2008, *AAP*, 488, L13
- [18] Schneider, P. C., Günther, H. M., & Schmitt, J. H. M. M. 2011, *AAP*, 530, A123
- [19] Soker, N. 2005, *AAP*, 435, 125
- [20] Stelzer, B., Hubrig, S., Orlando, S., et al. 2009, *AAP*, 499, 529
- [21] Tsujimoto, M., Koyama, K., Kobayashi, N., et al. 2004, *PASJ*, 56, 341
- [22] Woitas, J., Bacciotti, F., Ray, T. P., et al. 2005, *AAP*, 432, 149